5244 *Chem. Mater.* **2010,** *22,* 5244–5250
DOI:10.1021/cm101243m

CHEMISTRY OF MATERIALS
Article

Uniform, Spherical Bridged Polysilsesquioxane Nano- and Microparticles by a Nonemulsion Method

Li-Chih Hu,[†] Mariya Khiterer,[†] Shing-Jong Huang,[‡] Jerry Chun Chung Chan,[‡] Joseph R. Davey,[†] and Kenneth J. Shea*,[†]

[†]*Department of Chemistry, University of California, Irvine, 1102 Natural Sciences II, Irvine, California 92697-2025, and* [‡]*Department of Chemistry, National Taiwan University, No. 1, Sec. 4, Roosevelt Road, Taipei 106, Taiwan*

Received May 3, 2010. Revised Manuscript Received July 21, 2010

A nonemulsion method to prepare spherical, monodisperse nanoparticles of bridged polysilsesquioxanes was developed. This is the first method to fabricate uniform spherical bridged polysilsesquioxanes from monomers with low to moderate hydrophilicity. The average particle size can be systematically controlled from ~20 nm to ~1.5 μm. These particles have distinctive properties that include porosity without templating and buffering capacity. A mechanism for particle growth is proposed.

Introduction

Bridged polysilsesquioxanes (BPS)[1] are materials with silicon-oxide networks and organic bridging groups that are synthesized by sol−gel chemistry from organo-bridged bis-trialkoxysilanes [$(R'O)_3Si$-R-$Si(OR')_3$]. Following condensation, the organic and inorganic domains are dispersed at the molecular level. The organic group provides an opportunity to control bulk properties such as refractive index, optical clarity, hydrophobicity, dielectric constant, thermal stability[2] and chemical function.[3] Moreover, as compared to organic modified silica or ceramics[4] synthesized from R-$Si(OR)_3$, the organic group serves as a spacer between two $Si-O_{1.5}$ linkages, often providing significant and well-modulated porosity, with "inner surfaces" of up to ~1000 m^2/g.[1]

Recent developments for preparing functional materials as spherical micro or nanoparticles have broadened the potential applications and enhanced the performance of these materials. Small, uniform spherical particles are widely used in separations,[5] for drug and gene delivery,[6] bioimaging,[7] catalysis,[8] and for optical,[9] electronic,[10] and magnetic[11] applications. Recently, BPS were also prepared as xerogel nanoparticles by self-assembly[12] or by an emulsion method.[13] These nanoparticles were used as

*Corresponding author. E-mail: kjshea@uci.edu.

(1) (a) Shea, K. J.; Loy, D. A. *Chem. Mater.* **2001**, *13*, 3306–3319. (b) Shea, K. J.; Loy, D. A.; Webster, O. *J. Am. Chem. Soc.* **1992**, *114*, 6700–6710.
(2) Shea, K. J.; Moreau, J.; Loy, D. A.; Corriu, R. J. P.; Boury, B. *Funct. Hybrid Mater.* **2004**, *50*, 50–85.
(3) Zhao, L.; Vaupel, M.; Loy, D. A.; Shea, K. J. *Chem. Mater.* **2008**, *20*, 1870–1876.
(4) Wright, J. D.; Sommerdijk, N. A. J. M. In *Sol−Gel Materials. Chemistry and Applications*; Phillips, D., O'Brien, P., Roberts, S., Eds.; CRC Press: New York, 2001; Vol. *4*, pp 43−53.
(5) (a) Unger, K. K.; Kumar, D.; Grun, M.; Buchel, G.; Ludtke, S.; Adam, T.; Schumacher, K.; Renker, S. *J. Chromatogr., A* **2000**, *892*, 47–55. (b) Smith, J. E.; Wang, L.; Tan, W. T. *TrAC, Trends Anal. Chem.* **2006**, *25*, 848–855. (c) Guihen, E.; Glennon, J. D. *Anal. Lett.* **2003**, *36*, 3309–3336.
(6) (a) Barbe, C. B.; John; Kong, L.; Finnie, K.; Lin, H. Q.; Larkin, M.; Calleja, S.; Bush, A.; Calleja, G. *Adv. Mater.* **2004**, *16*, 1959–1966. (b) Singh, M.; Briones, M.; Ott, G.; O'Hagan, D. *Proc. Natl. Acad. Sci. U.S.A.* **2000**, *97*, 811–816. (c) Roy, I.; Ohulchanskyy, T. Y.; Bharali, D. J.; Pudavar, H. E.; Mistretta, R. A.; Kaur, N.; Prasad, P. N. *Proc. Natl. Acad. Sci. U.S.A.* **2005**, *102*, 279–284. (d) Bharali, D. J.; Klejbor, I.; Stachowiak, E. K.; Dutta, P.; Roy, I.; Kaur, N.; Bergey, E. J.; Prasad, P. N.; Stachowiak, M. K. *Proc. Natl. Acad. Sci. U.S.A.* **2005**, *102*, 11539–11544. (e) Roy, I.; Ohulchanskyy, T. Y.; Pudavar, H. E.; Bergey, E. J.; Oseroff, A. R.; Morgan, J.; Dougherty, T. J.; Prasad, P. N. *J. Am. Chem. Soc.* **2003**, *125*, 7860–7865. (f) Wang, C.; Ge, Q.; Ting, D.; Nguyen, D.; Shen, H. R.; Chen, J. Z.; Eisen, H. N.; Heller, J.; Langer, R.; Putnam, D. *Nat. Mater.* **2004**, *3*, 190–196. (g) Sengupta, S.; Eavarone, D.; Capila, I.; Zhao, G. L.; Watson, N.; Kiziltepe, T.; Sasisekharan, R. *Nature* **2005**, *436*, 568–572. (h) Haag, R. *Angew. Chem., Int. Ed.* **2004**, *43*, 278–282. (i) Yoon, T. J.; Kim, J. S.; Kim, B. G.; Yu, K. N.; Cho, M. H.; Lee, J. K. *Angew. Chem., Int. Ed.* **2005**, *44*, 1068–1071. (j) Yan, A. H.; Lau, B. W.; Weissman, B. S.; Kulaots, I.; Yang, N. Y. C.; Kane, A. B.; Hurt, R. H. *Adv. Mater.* **2006**, *18*, 2373.
(7) (a) Santra, S.; Bagwe, R. P.; Dutta, D.; Stanley, J. T.; Walter, G. A.; Tan, W.; Moudgil, B. M.; Mericle, R. A. *Adv. Mater.* **2005**, *17*, 2165–2169. (b) Lee, J.-H.; Jun, Y.-W.; Yeon, S.-I.; Shin, J.-S.; Cheon, J. *Angew. Chem., Int. Ed.* **2006**, *45*, 8160–8162.
(8) (a) Beydoun, D.; Amal, R.; Low, G.; McEvoy, S. *J. Nanopart. Res.* **1999**, *1*, 439–458. (a) Zhong, C. J.; Maye, M. M. *Adv. Mater.* **2001**, *13*, 1507.
(9) (a) Zhu, M. Q.; Zhu, L. Y.; Han, J. J.; Wu, W. W.; Hurst, J. K.; Li, A. D. Q. *J. Am. Chem. Soc.* **2006**, *128*, 4303–4309. (b) Ow, H.; Larson, D. R.; Srivastava, M.; Baird, B. A.; Webb, W. W.; Wiesner, U. *Nano Lett.* **2005**, *5*, 113–117.
(10) (a) Kaltenpoth, G.; Himmelhaus, M.; Slansky, L.; Caruso, F.; Grunze, M. *Adv. Mater.* **2003**, *15*, 1113–1118. (b) Jang, J.; Nam, Y.; Yoon, H. *Adv. Mater.* **2005**, *17*, 1382–1386.
(11) (a) Yi, D. K.; Lee, S. S.; Papaefthymiou, G. C.; Ying, J. Y. *Chem. Mater.* **2006**, *18*, 614–619. (b) Lu, A. H.; Salabas, E. L.; Schuth, F. *Angew. Chem., Int. Ed.* **2007**, *46*, 1222–1244. (c) Toprak, M. S.; McKenna, B. J.; Mikhaylova, M.; Waite, J. H.; Stucky, G. D. *Adv. Mater.* **2007**, *19*, 1362. (d) Ma, Z. Y.; Guan, Y. P.; Liu, H. Z. *J. Polym. Sci., Part A: Polym. Chem* **2005**, *43*, 3433–3439. (e) Xu, H.; Cui, L. L.; Tong, N. H.; Gu, H. C. *J. Am. Chem. Soc.* **2006**, *128*, 15582–15583. (f) Lu, C. W.; Hung, Y.; Hsiao, J. K.; Yao, M.; Chung, T. H.; Lin, Y. S.; Wu, S. H.; Hsu, S. C.; Liu, H. M.; Mou, C. Y.; Yang, C. S.; Huang, D. M.; Chen, Y. C. *Nano Lett.* **2007**, *7*, 149–154.
(12) Zhao, L.; Loy, D. A.; Shea, K. J. *J. Am. Chem. Soc.* **2006**, *128*, 14250.
(13) Khiterer, M.; Shea, K. J. *Nano Lett.* **2007**, *7*, 2684–2687.

Published on Web 08/11/2010

photodeformable materials[11] or components in a solid-state electrochromic device.[14] However, the water-in-oil emulsion method is only suitable for ionic and water-soluble monomers since hydrophobic monomers become amphiphilic after hydrolysis, and are not constrained in micelles. Furthermore, the rational design of BPS monomers which can self-assemble into nanoparticles may have a very limited scope. Since most bridged silane monomers are water-insoluble, a new general method is needed to prepare BPS as uniform, spherical particles.

The Stöber process[15] yields monodisperse spherical nonporous silica particles by the hydrolysis and condensation of $Si(OEt)_4$ in alcoholic solutions of ammonia and water. Organically modified silica particles can be prepared by the Stöber process[16] in which aqueous ammonium hydroxide (without alcohol) is used as solvent. During the reaction, the monomer "droplets" are gradually consumed, and a turbid suspension of organic-silica particles emerge in the aqueous phase. These results suggest that "Stöber-like" aqueous ammonia conditions may be suited to prepare spherical BPS particles from water-insoluble bridged silane monomers.

Experimental Section

Materials. All monomers were purchased from Gelest, Inc. Ammonium hydroxide was purchased from Fisher Scientific, diluted to 1.5 M stock solution, and titrated by 0.100 M HCl standard solution (Fisher Scientific). 1-Propanol was purchased from Aldrich. All were used as received unless otherwise specified.

Particle Synthesis: General Procedures. To a 7 mL sample vial was added 1 M NH_3 as a mixture of 1.5 M $NH_{3(aq)}$, H_2O, and 1-PrOH (2.7 mL total, see Table S1 in the Supporting Information). The solution was preheated to the reaction temperature (60 °C, unless otherwise specified; titration showed the remaining [NH_3] after preheat is generally 0.95−0.97 M). To the solution was added 2.8 mmol of bridged silane monomer. The biphasic mixture was stirred vigorously for 30 min, after which immiscible monomer could not be visually detected. The resulting suspension was allowed to cool to r.t., aged overnight, and then dialyzed against water (3 L) in regenerated cellulose tubing (12−14K cut off, Fisherbrand) for 24 h (the water was changed at 6 h). Dialyzed suspensions were kept under ambient temperature. For yield calculation and evaluation of dry particle properties, suspensions were dialyzed against MeOH (300 mL) in regenerated cellulose tubing for 24 h (the MeOH was changed at 3 and 6 h) and dried by rotavap followed by drying under high vacuum (see the Supporting Information).

Scanning Electron Microscopy (SEM). SEM was performed on a Zeiss Ultra 55 CDS field-emission scanning electron microscope. Specimens were prepared by drop coating diluted and sonicated water suspensions of particles onto silicon wafers, followed by drying overnight under room temperature and atmosphere. Typical acceleration voltages used were 2.5−5 kV. Resulting images were analyzed by ImagePro AMS 6.0 for particle sizes; > 100 particles were measured for each sample.

Light Scattering Analysis. Dynamic light scattering (DLS) and zeta potential measurements were carried out on a Malvern Zetasizer Nano ZS light scattering analyzer. Nanoparticle suspensions for DLS and zeta potential measurements were dialyzed against water, diluted with water (unless otherwise specified) and sonicated for 30 min before measurement; suspensions with average particle diameters under 100 nm were filtered through PVDF syringe filters (pore size 200 nm, purchased from Nalge Nunc Int.). Default settings, including automatic optical parameter selection, were used for both experiments.

Gas Adsorption Analysis. Nitrogen adsorption was measured on a Quantachrome Autosorb-1 at 77K, P/P_0 ranged from 1×10^{-6} to 0.995. Thirty to one-hundred milligrams of dried particle powder was outgassed at 160 °C until the outgas pressure rise was below 20 μmHg/min prior to analysis. The resulting isotherms were converted to surface area and pore size distribution profile with multipoint BET and QSDFT adsorption model fitting (Quantachrome Autosorb-1 for Windows software, V 1.55), respectively.

Solid-State NMR. All solid-state NMR experiments were carried out on a Bruker 300 DSX NMR spectrometer equipped with a 7-mm double-resonance magic-angle-spinning (MAS) probe head. Single-pulse ^{29}Si MAS experiments were accumulated with 300 - 600 free induction decays (FIDs) with the $\pi/3$ pulse of 6 μs and the repetition time of 180 s. In the case of cross-polarization (CP) experiments, the radiofrequency (rf) strength for ^1H was 25 kHz, whereas the Hartmann−Hahn match condition for ^{29}Si was optimized based on the signal of sodium 3-(trimethylsilyl)-1-propanesulfonate hydrate. The CP contact time was 2 ms.

Results and Discussion

Preliminary Trials. When "0.1M" (calculated as if it were fully dissolved) 1,4-bis(triethoxysilyl)benzene was added to 1.0 M aqueous ammonia at 60 ^{o}C under vigorous stirring, the monomer droplets were not completely consumed even after 3 days. The water phase was opalescent, suggesting the presence of colloids. SEM images taken following drying a drop of the water phase on a Si wafer, revealed particles with an average diameter of ~25 nm. Prolonged exposure to the electron beam resulted in particle degradation, suggesting a very low degree of condensation. Changing the monomer to 1,8-bis(triethoxysilyl)-octane gave a similar result. 1,2-Bis(triethoxysilyl)ethane was used to test whether its higher water solubility facilitates the reaction. However, using the above conditions, no particles were observed under SEM from the dried homogeneous reaction mixture after ~2 h of reaction. The reaction mixture turned into a transparent bulk gel after several days. (Table 1)

Partially hydrolyzed trimethoxysilyl species have greater water solubility and the hydrolysis rate of trimethoxysilyl group is several orders of magnitude faster than the triethoxysilyl group.[13] An attempt using bis(trimethoxysilylethyl)benzene (**1**, ~85% para isomer) under the above

(14) Jain, V.; Khiterer, M.; Montazami, R.; Yochum, H.; Shea, K. J.; Heflin, R. *ACS Appl. Mater. Interfaces* **2009**, *1*, 83–89.
(15) Stober, W.; Fink, A.; Bohn, E. *J. Colloid Interface Sci.* **1968**, *26*, 62–69.
(16) (a) Choi, J. Y.; Kim, C. H.; Kim, D. K. *J. Am. Ceram. Soc.* **1998**, *81*, 1184–1188. (b) Katagiri, K.; Hasegawa, K.; Matsuda, A.; Tatsumisago, M.; Minami, T. *J. Am. Ceram. Soc.* **1998**, *81*, 2501–2503. (c) Matsuda, A.; Sasaki, T.; Tanaka, T.; Tatsumisago, M.; Minami, T. *J. Sol−Gel Sci. Technol.* **2002**, *23*, 247–252. (d) Liu, S. M.; Lang, X. M.; Ye, H.; Zhang, S. J.; Zhao, J. Q. *Eur. Polym. J.* **2005**, *41*, 996–1001. (e) Arkhireeva, A.; Hay, J. N. *J. Mater. Chem.* **2003**, *13*, 3122–3127. (f) Arkhireeva, A.; Hay, J. N.; Lane, J. M.; Manzano, M.; Masters, H.; Oware, W.; Shaw, S. J. *J. Sol−Gel Sci. Technol.* **2004**, *31*, 31–36. (g) Nakamura, M.; Ishimura, K. *Langmuir* **2008**, *24*, 12228–12234. (h) Nakamura, M.; Ishimura, K. *Langmuir* **2008**, *24*, 5099–5108. (i) Nakamura, M.; Ishimura, K. *J. Phys. Chem. C* **2007**, *111*, 18892–18898.

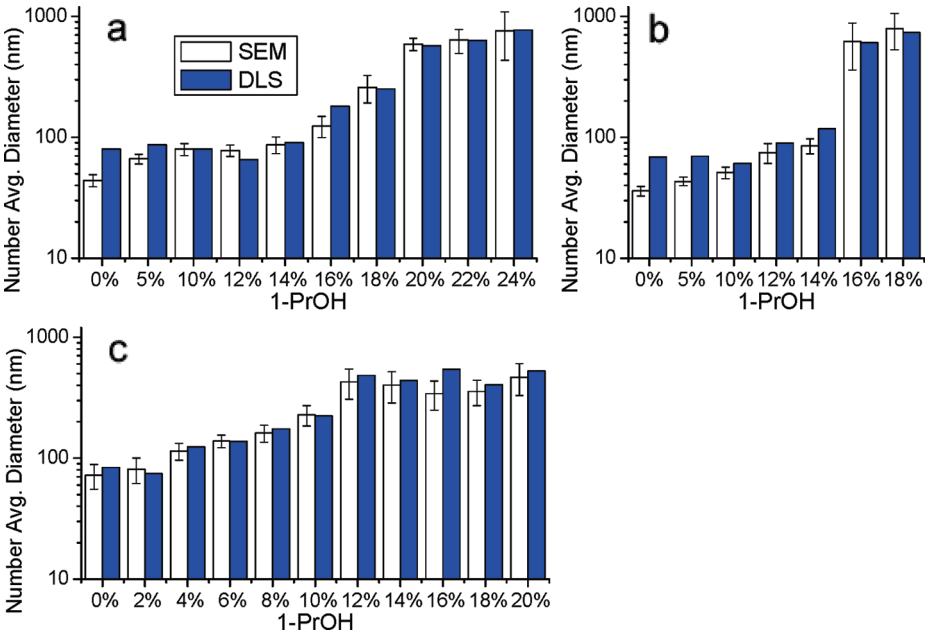

Figure 1. Size of BPS nanoparticles (a) **1P**, (b) **2P**, and (c) **3P** as a function of H_2O 1-PrOH ratio in the polymerization process.

Table 1. Preliminary Trials of Modified Stöber Methods for Preparing BPS Nanoparticles;. In Entries 1 and 2, Unreacted Monomer Droplets Were Observed after 3 Days

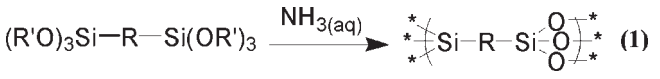

Entry	R	R'	Results
1		Et	Low extent of reaction
2	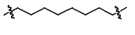	Et	Low extent of reaction
3		Et	Bulk gelation
4		Me	NP formed (**1P**, 44±5 nm)

conditions, resulted in full consumption of monomer droplets and formation of nanoparticles (44 ± 5 nm); the NPs formed were stable under e-beam in SEM observation.

This observation suggests the higher monomer reactivity and resulting increased reactive soluble monomer concentration contributed by trimethoxysilyl groups could be important for synthesizing spherical particles of bridged polysilsesquioxanes. The following studies build upon this finding with monomers containing two trimethoxysilyl groups.

Particle Synthesis. Reports of the "Stöber-like" process for organic modified silica particles[13] emphasize monomer concentration as a key to nanoparticle size control. However, when the concentration of **1** was increased from 0.1 to 0.2 M, particle size did not change significantly (43 ± 5 nm). One important observation however, was that the droplets of monomer **1** were not consumed until ~1.5 h after the reaction was initiated. This observation suggests that the "effective concentration" of monomer in the water phase is limited not only by the rate of hydrolysis but by the intrinsic solubility of the monomer. To test the hypothesis, we employed a water-organic solvent mixture. The solubility of monomers was adjusted by altering the percentage of organic solvent while keeping the ammonia concentration at 1M. 1-Propanol was chosen as the organic solvent.[17] These modified conditions resulted in formation of spherical uniform particles. Furthermore, particle size (measured by dynamic light scattering (DLS) and scanning electron microscopy (SEM)) could be controlled by the alcohol content. The results are summarized in Figure 1a. SEM analysis shows **1P** particles produced with 0−12% 1-PrOH are monodisperse (~11% relative standard deviation of diameter). The size uniformity was slightly less as the 1-PrOH percentage increased from 14 to 18% (15−25% RSD). Particles are again highly monodisperse with 20% 1-PrOH (11% RSD). A further increase of the 1-PrOH percentage (22−24%) results in some loss of monodispersity due to the emergence of smaller particles.

To test the generality of the method, we included hexyl-bridged monomer **2** and tertiary amine bridged monomer **3** in the study. The hypothesis of positive correlations with 1-PrOH content, monomer concentration, and particle size was supported by these experiments.

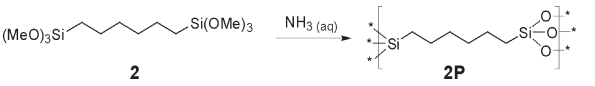

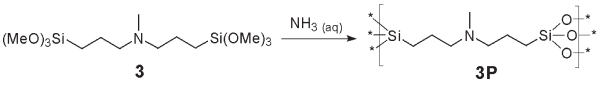

In pure aqueous ammonia, **2P** nanoparticles were less spherical with some fused clusters compared to **1P** nanoparticles, (Figure 2b). Increasing the 1-PrOH content from 0% to 10% resulted in not only larger particles,

(17) Reasons for choosing 1-PrOH as cosolvent: full miscibility with H_2O, similarity with H_2O in boiling point, hydrogen bonding characteristics, and polarity.

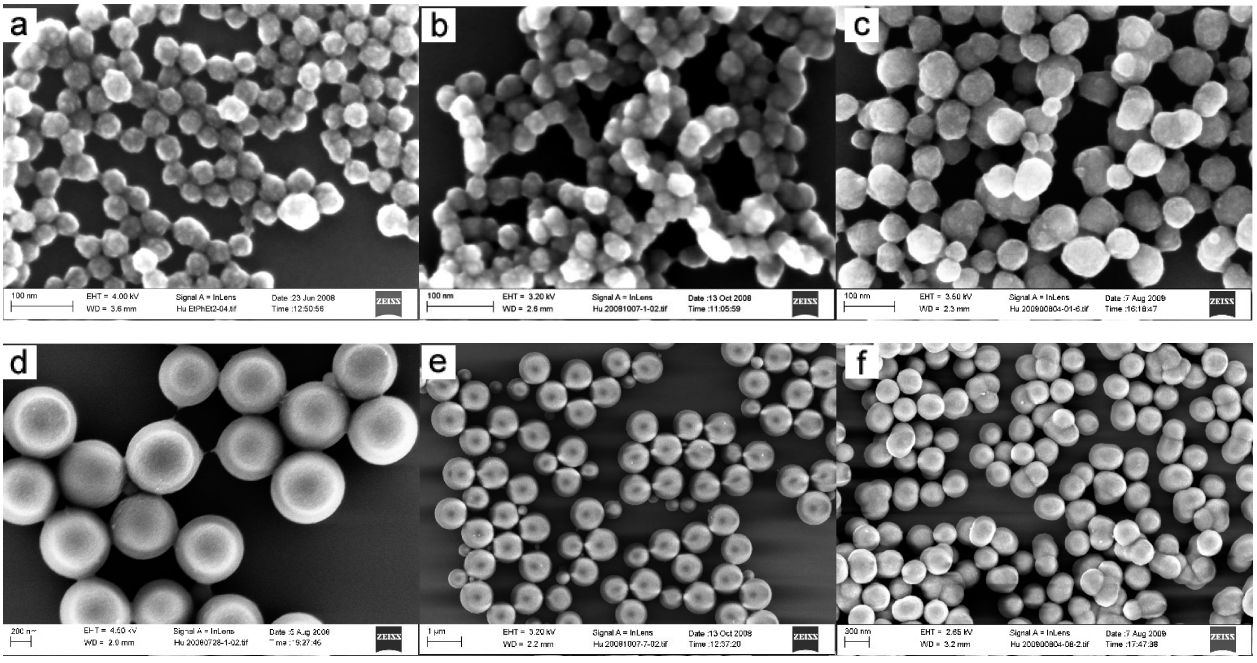

Figure 2. (a−c) Representative BPS NPs: (a) **1P**, (b) **2P**, and (c) **3P** synthesized in aqueous ammonia solution (0% 1-PrOH). (d−f) Example of "large" BPS NPs: (d) **1P**, (e) **2P**, and (f) **3P** synthesized in ammonia solution with (d) 20%, (e) 18%, and (f) 14% 1-PrOH. Scale bars represent (a−c) 100 nm, (d) 200 nm, (e) 1 μm, and (f) 300 nm.

but also a greater incidence of spherical rather than fused particles. Approximately 80 nm **3P** particles were formed in aqueous 1 M NH_3; increasing 1-PrOH concentration from 0 to 14% gradually increased particle diameters up to ~400 nm. Particle size does not change significantly with further increases in 1-PrOH concentration (Figure 1c).

For nanoparticles > 70 nm, the difference of particle sizes determined by DLS and SEM are generally small. Thus, there is little shrinkage of particles as a result of drying, which implies that the particles as formed are highly condensed. This is in contrast to bulk BPS gels of identical chemical composition, which undergo substantial shrinkage (~80%) upon drying to a xerogel.[18]

Particle Growth Mechanism. An apparent trend is observed for the synthesis of BPS NPs: as the 1-PrOH content increases, larger particles are formed. Particles can be synthesized with up to 20-fold size difference, simply by adjusting the 1-PrOH content. The time needed for full consumption of monomer droplets and the appearance of turbidity decreases with increasing 1-PrOH percentage. Generally, at 60 °C, monomer **1** takes less than 20 min in 10% 1-PrOH and less than 3 min in 20% 1-PrOH to be fully consumed. Importantly, we can correlate the increase of monomer dissolution with the increase of resulting particle sizes.

Models used to discuss the growth of silica particles under Stöber conditions[19] may help to explain this result. There are two well-accepted particle growth models for the process: "monomer addition"[20] and "controlled aggregation."[21] The condensation of partially hydrolyzed soluble monomers results in nucleation. In the first model, the particle grows only by addition of hydrolyzed monomers to surface $Si-O^-$ groups; in the latter model, once the particles have reached a certain size, they grow only by aggregation. In the SEM images, the spheres appear to be composed of smaller nanoparticles with diameters approximately 5−10 nm (Figure 3), suggesting that the "controlled aggregation" model may be important for the growth of BPS nanoparticles.

Particle growth by aggregation is supported by the following. As the monomer solubility increases with a higher concentration of 1-PrOH, the number of particle "seeds" or nucleation sites in the water phase is expected to increase. If the "monomer addition" mechanism were dominating, the final particle size would be smaller in this case, because of the larger number of nucleation sites. The model of "controlled aggregation" explains the experimental trend better: if a large number of nucleation sites are produced in a short time in a solution rich in 1-PrOH, they have greater probability to chemically aggregate before their surface silanol groups condense with adjacent ones (Figure 4). This is expected to result in larger particles in solutions rich in 1-PrOH. It is noted that SEM images of particles have smoother surfaces than a pure aggregate of small spheres. The "monomer addition" mechanism, which is believed to contribute to smoothing the particle surface,[22] may still play a role in the particle growth.

Colloidal Charge. The growth of particles from monomer **3** is particularly interesting since the organic fragment, a

(18) Loy, D. A.; Shea, K. *J. Chem. Rev.* **1995**, *95*, 1431–1442.
(19) Van Blaaderen, A.; Van Geest, J.; Vrij, A. *J. Colloid Interface Sci.* **1992**, *154*, 481–501.
(20) (a) Matsoukas, T.; Gulari, E. *J. Colloid Interface Sci.* **1988**, *124*, 252. (b) Matsoukas, T.; Gulari, E. *J. Colloid Interface Sci.* **1989**, *132*, 13. (c) Matsoukas, T.; Gulari, E. *J. Colloid Interface Sci.* **1991**, *145*, 557.
(21) (a) Kim, S.; Zukoski, C. F. *J. Colloid Interface Sci.* **1990**, *139*, 198. (b) Bogush, G. H.; Zukoski, C. F., IV. *J. Colloid Interface Sci.* **1991**, *142*, 1. (c) Bogush, G. H.; Zukoski, C. F., IV. *J. Colloid Interface Sci.* **1991**, *142*, 17.
(22) Green, D. L.; Lin, J. S.; Lam, Y.-F.; Hu, M. Z.-C.; Schaefer, D. W.; Harris, M. T. *J. Colloid Interface Sci.* **2003**, *266*, 346–358.

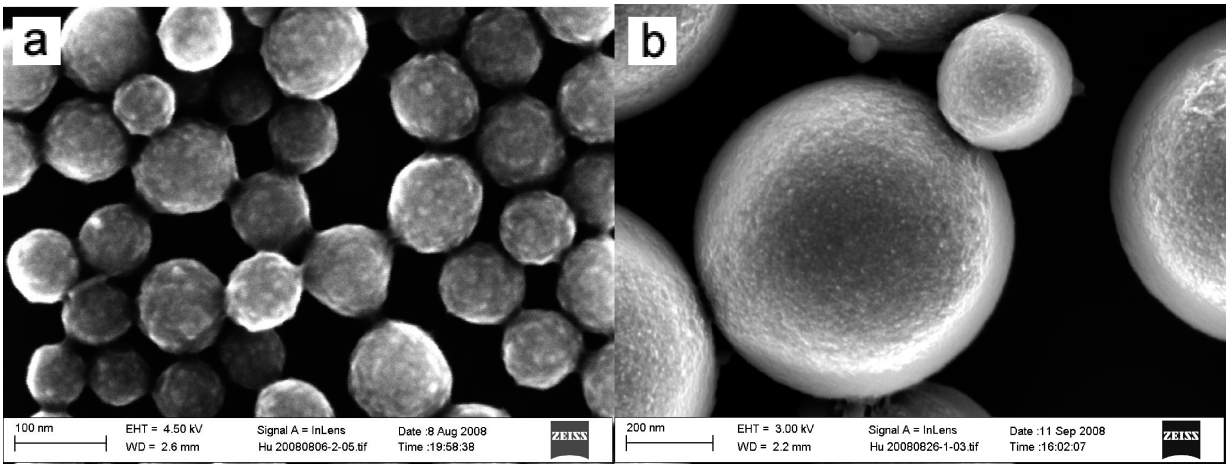

Figure 3. Close look at **1P** nanoparticles: (a) 70 and (b) 800 nm.

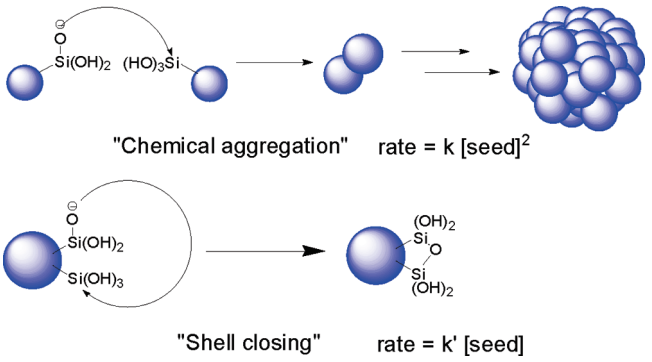

Figure 4. Competitive mechanisms for particle growth and size limitation.

tertiary amine, can bear a positive charge that can influence particle stability and the growth process. Upon close examination, some of the **3P** nanoparticles appear to be comprised some "twinned" particles (Figures 2c, 2f, and S3). The zeta potential of diluted reaction solutions of **3P** particles is approximately −20 to −30 mV (Table 2). Colloidal particles with zeta potentials in this region typically have marginal colloidal stability. In contrast, hydrocarbon-bridged **1P** and **2P** particles exhibit zeta potentials (−45 to −50 mV) sufficient to support stable colloidal suspensions. Thus, **3P** particles would be expected to have a stronger tendency than those with neutral bridging groups, to aggregate at all stages of the growth process; the growth can continue on the aggregated particles, leading in some cases to their "twinned" appearance (Figure 5).

The chemical composition of NP **3P** can help explain its suggested mechanism of formation and the medium effect on its zeta potential. Tertiary amines have K_b values almost 1 order of magnitude lower than ammonia, thus they are partially protonated even in ammonia solution. Under dilute basic conditions, the core exhibits positive charge that partially compensates the negative charge of deprotonated surface silanols. This can account for their less negative zeta potential. The positive charge in the core is dominant after dialysis against water. Buffering capacity is observed upon acidification (Table 2), a behavior

Table 2. Zeta Potential of 3P Nanoparticles Tuned by Different Acid−Base Conditions

treatment of rxn mixture	pH	ζ potential (mV)
diluted w/1 M NH_3	11.1	−32 ± 6
diluted w/H_2O	10.3	−19 ± 5
dialyzed w/H_2O	8.9	+23 ± 7
dialyzed w/H_2O,	7.4 [a]	+48 ± 5 [a]
then added HCl	6.5 [b]	+49 ± 6 [b]

Amount of HCl: [a] 3 mol % of monomer; [b] 30 mol % of monomer.

similar to poly(ethylene imine) functionalized nanoparticles.[23] The buffering effect promotes endosomal escape[24] of NPs, enhancing their drug and DNA delivery efficiency toward cells. Because this buffering capacity is an intrinsic property of **3P** nanoparticles while still retaining the ability for surface modification and labeling, **3P** particles may be promising drug and DNA carriers. The interaction between **3P** NPs and biological macromolecules and cells is under investigation.

Other Factors that Influence Particle Size. With 22% 1-PrOH, increasing the concentration of monomer **1** up to 0.15 M resulted in monodisperse (∼10% relative standard deviation) particles up to 1.5 μm. A further increase in [monomer **1**] and [1-PrOH] resulted in bimodal particle size distribution and polydisperse microparticles, respectively (see Table 3 and Figures S4 − S7 in the Supporting Information).

To further establish the relationship between particle size and monomer concentration, BPS NPs **1P** were synthesized in 1 M aqueous NH_3 but at monomer concentrations of 0.05, 0.02, and 0.01 M. The results show that this variable can be successfully applied to prepare particles as small as ∼20 nm. Comparison between size determined by DLS and SEM has shown that the extent of particle aggregation in water suspensions is low under most conditions (Figure 6).

(23) Rosenholm, J. M.; Meinander, A.; Peuhu, E.; Niemi, R.; Eriksson, J. E.; Sahlgren, C.; Lindén, M. *ACS Nano* **2009**, *3*, 197–206.
(24) (a) Godbey, W. T.; Wu, K. K.; Mikos, A. G. *J. Controlled Release* **1999**, *60*, 149–160. (b) Lim, Y. B.; Kim, S. M.; Lee, Y.; Lee, W. K.; Yang, T.-G.; Lee, M.-J.; Suh, H.; Park, J.-S. *J. Am. Chem. Soc.* **2001**, *123*, 2460–2461.

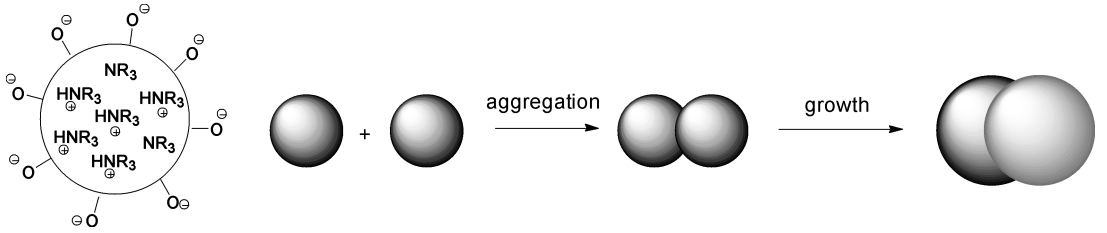

Figure 5. Schematic explanation of morphology of particle **3P**.

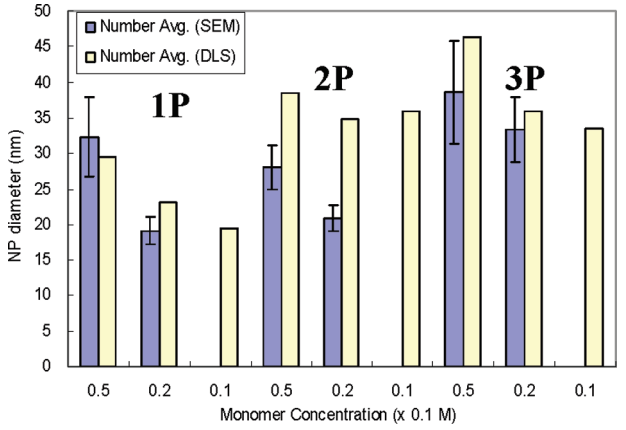

Figure 6. BPS nanoparticle size prepared at monomer concentration < 0.1 M.

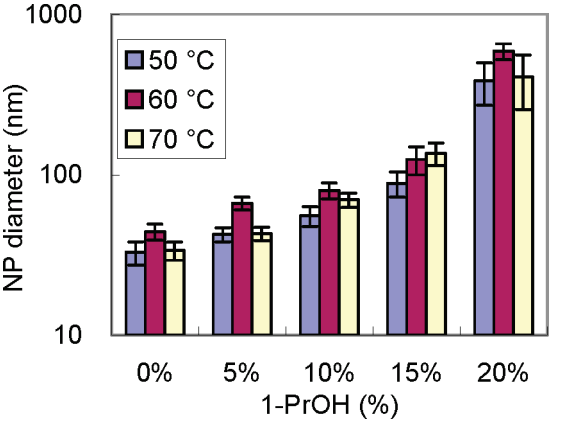

Figure 7. Comparison of **1P** particle size (determined by SEM) as a function of temperature and 1-propanol content.

Table 3. Size of 1P Particles (μm) As a Function of [1-PrOH] and [monomer 1]

	[1-PrOH]		
[monomer 1] (M)	20%	22%	24%
0.12	0.83	1.1	0.5−4[c]
0.135	1.2[a]	1.3	0.5−4[c]
0.15	1.2[b]	1.5	0.5−4[c]
0.20	0.81[b]	1.2[b]	0.2−3[c]

[a] Small fractions of smaller particles (100−300 nm) were detected. [b] Considerable fractions of smaller particles (100−300 nm) were detected. [c] Highly polydisperse particles.

Table 4. Porosimetry and Solid-State NMR Data of BPS NPs of Various Composition and Sizes

entry	material	1-PrOH (%)	D_{avg} (nm, SEM)	surface area (m^2/g)	pore volume (mL/g)	degree of condensation (%)
1	**1P**	0	44	204	0.60	82.4[a], 81.4[b]
2	**1P**	20	590	12	0.03	82.9[a]
3	**2P**	0	36	231	0.66	82.7[a], 83.7[b]
4	**2P**	16	620	38	0.14	80.5[a]
5	**3P**	0	84	137	0.75	82.1[a], 86.8[b]
6	**3P**	14	440	22	0.11	80.1

[a] From cross-polarization experiments. [b] From single-pulse experiments.

To test the effect of temperature (which can influence both reaction rate and monomer solubility), we examined the synthesis of **1P** from **1** at 50 and 70 °C with various water−alcohol ratios as solvent. Generally, the particles prepared at 60 °C are larger and more uniform in size (Figure 7). Within this range, the influence of temperature on particle size is relatively minor.

Surface Area and Porosity. All nanoparticles exhibit a small component of microporosity (pore diameter < 2 nm), which contributes to the total surface area (4−15 m^2/g for "large" NPs, 20−40 m^2/g for "small" NPs, Table 3). NPs synthesized in NH_3 solution with 0% 1-PrOH also have considerable mesoporosity, which we suggest is attributed in part to the interstitial spaces between particles (see Table 4 and Figure S9). Thus, these "small" NPs can be also considered as bulk materials or clusters with high surface area and dual (meso- and micro-) porosity.

Solid-State NMR Spectroscopy. The spectral resolution (^{29}Si CP/MAS solid-state NMR) of the particles increases in the order **1P** < **3P** < **2P**. **2P** and **3P** NPs synthesized without 1-PrOH have a higher degree of condensation than particles of the same chemical composition but synthesized with 1-PrOH as cosolvent. This trend, however, is not observed for **1P**, perhaps due to the greater error in calculating the condensation because of lower spectral resolution. Single-pulse experiments, only done on entries 1, 3, and 5 in Table 4, suggests that the degree of condensation of particles is higher with monomers with a greater intrinsic solubility in water (**3P** > **2P** > **1P**) (see Figure S10 in the Supporting Infomration and Table 4).

Conclusion

We have developed a method to prepare spherical, monodisperse nanoparticles of bridged polysilsesquioxanes. The average particle size can be systematically controlled between ~20 nm to ~1.5 μm. The modified Stöber process is suitable for organic molecules with low to moderate hydrophilicity containing two trimethoxysilyl groups.[1,13,25] Distinctive properties such as porosity without templating

and buffering capacity were observed. This technique enables the synthesis of spherical functional nano- and micrometer- sized hybrid materials with a range of chemical, physical, and mechanical compositions.

(25) (a) Murata, M.; Yamasaki, H.; Ueta, T.; Nagata, M.; Ishikura, M.; Watanabe, S.; Masuda, Y. *Tetrahedron* **2007**, *63*, 4087–4094. (b) Cerveau, G.; Chappellet, S.; Corriu, R. J. P.; Dabiens, B. *J. Organomet. Chem.* **2001**, *626*, 92–99.

Acknowledgment. We thank Shiseido Co. Ltd for support of this research. L.-C.H. is grateful for a fellowship from Lawrence Livermore National Laboratory.

Supporting Information Available: A description of particle synthesis, SEM images of particles, particle size analysis data, N_2 adsorption analysis data and solid-state NMR data. This material is available free of charge via the Internet at http://pubs.acs.org.